

2-19-2009

# Simulation of the Middle Miocene climate optimum: implications for future climate

Y. You

*Univ. of Sydney*

Matthew Huber

*Purdue, huber@purdue.edu*

D. R. Müller

*Univ. of Sydney*

C. J. Poulsen

*Univ. of Michigan*

J. Ribbe

*University of Southern Queensland, Toowoomba, Queensland, Australia*

Follow this and additional works at: <http://docs.lib.purdue.edu/easpubs>

---

## Repository Citation

You, Y.; Huber, Matthew; Müller, D. R.; Poulsen, C. J.; and Ribbe, J., "Simulation of the Middle Miocene climate optimum: implications for future climate" (2009). *Department of Earth, Atmospheric, and Planetary Sciences Faculty Publications*. Paper 92.  
<http://dx.doi.org/10.1029/2008GL036571>

## Simulation of the Middle Miocene Climate Optimum

Y. You,<sup>1,2</sup> M. Huber,<sup>3</sup> R. D. Müller,<sup>2</sup> C. J. Poulsen,<sup>4</sup> and J. Ribbe<sup>5</sup>

Received 4 November 2008; revised 20 December 2008; accepted 26 January 2009; published 19 February 2009.

[1] Proxy data constraining land and ocean surface paleotemperatures indicate that the Middle Miocene Climate Optimum (MMCO), a global warming event at  $\sim 15$  Ma, had a global annual mean surface temperature of  $18.4^{\circ}\text{C}$ , about  $3^{\circ}\text{C}$  higher than present and equivalent to the warming predicted for the next century. We apply the latest National Center for Atmospheric Research (NCAR) Community Atmosphere Model CAM3.1 and Land Model CLM3.0 coupled to a slab ocean to examine sensitivity of MMCO climate to varying ocean heat fluxes derived from paleo sea surface temperatures (SSTs) and atmospheric carbon dioxide concentrations, using detailed reconstructions of Middle Miocene boundary conditions including paleogeography, elevation, vegetation and surface temperatures. Our model suggests that to maintain MMCO warmth consistent with proxy data, the required atmospheric  $\text{CO}_2$  concentration is about 460–580 ppmv, narrowed from the most recent estimate of 300–600 ppmv. **Citation:** You, Y., M. Huber, R. D. Müller, C. J. Poulsen, and J. Ribbe (2009), Simulation of the Middle Miocene Climate Optimum, *Geophys. Res. Lett.*, *36*, L04702, doi:10.1029/2008GL036571.

### 1. Introduction

[2] The Middle Miocene Climate Optimum (MMCO) occurred at about 15 Ma and represents a geologically recent warming event unrelated to human activity that may mirror future climate change in terms of the average global surface temperature increase. *Flower and Kennett* [1994] estimate that the MMCO was associated with a mid-latitude warming of about  $6^{\circ}\text{C}$  relative to the present. However, the cause of the MMCO warming and the role and scale of atmospheric carbon dioxide ( $\text{CO}_2$ ) is vigorously debated. Estimates of Middle Miocene paleo- $\text{CO}_2$  range from glacial levels to nearly twice the modern value. On the basis of paleosol  $\delta^{13}\text{C}$ , *Cerling* [1991] estimates a mean mid-Miocene atmospheric  $\text{CO}_2$  concentration of 700 ppmv. Using stomatal indices from fossil leaves, *Royer et al.* [2001] and *Kürschner et al.* [2008] obtain intermediate values ranging from somewhat less than modern (307–316 ppmv) to higher-than-modern (500 ppmv)  $\text{CO}_2$  levels. In contrast, marine  $\text{CO}_2$  proxy records indicate much lower values. *Pagani*

*et al.* [1999] calculate  $\text{CO}_2$  levels of 180–290 ppmv, low values which were confirmed by *Pearson and Palmer* [2000]. The low  $\text{CO}_2$  estimates suggest that  $\text{CO}_2$  and surface temperature were not linked during the MMCO, and raises the possibility of a  $\text{CO}_2$ -temperature decoupling during other times in Earth history.

[3] To date the warmth of the MMCO under low  $\text{CO}_2$  levels has not been reproduced by climate models. Modeling of the MMCO has proven to be extremely difficult due to a lack of detailed global boundary and initial conditions, sparse proxy data, and disparate  $\text{CO}_2$  concentrations. Here we use the latest NCAR Atmosphere Model CAM3.1 and Land Model CLM3.0 coupled to a slab ocean forced with realistic Miocene boundary conditions, including vegetation, elevation, SST forcing and calculated ocean heat fluxes based on proxies, and orbital parameters, to narrow the likely range of MMCO atmospheric  $\text{CO}_2$  concentrations.

### 2. Data and Methods

[4] The SSTs based on oxygen stable isotopes  $\delta^{18}\text{O}$  for the MMCO are scarce. Moreover, the distribution of proxy SSTs is not uniform, but skewed toward the low latitudes of the northern hemisphere. A summary of all available paleo-SSTs demonstrates a very large scatter of tropical SSTs between about  $15^{\circ}$  and  $30^{\circ}\text{C}$ . A Gaussian best-fit to the data ranges from  $0$ – $5^{\circ}\text{C}$  at high latitudes to about  $23^{\circ}\text{C}$  at low latitudes, nearly  $5^{\circ}\text{C}$  lower than present (see Figures 1a and 2).

[5] The approach we take is to use reconstructed Miocene SST gradients to estimate meridional ocean heat fluxes. This is necessary because slab ocean models do not include dynamics, and the modern ocean heat flux may not be appropriate for Miocene [*von der Heydt and Dijkstra*, 2006]. First, we prescribe zonal constant SST constructed from a Gaussian best fit to all proxy data with a lowest equator-to-pole gradient called LGRAD, equivalent to the so called “cool tropical paradox”. Following the method of *Huber et al.* [2003], we then modify the LGRAD by creating a new SST gradient using the maximum SSTs in the tropics, but modified high latitudes temperatures to maintain the global mean SST of  $20.6^{\circ}\text{C}$ . Here we choose two modified zonal SST profiles, one matching the present SST called MGRAD with a medium equator-to-pole gradient and another HGRAD with equatorial SST  $2$ – $3^{\circ}\text{C}$  higher than present [*Graham*, 1994]. As a result, three scenarios of initial SST forcing are specified. Monthly SSTs are calculated based on present seasonality (see SM\_JJA and SM\_DJF for summer and winter in Figure 1a).

[6] The models we employ are the latest NCAR CAM3.1 and CLM3.0 coupled to a slab ocean model with a T31 resolution ( $\sim 3.75^{\circ} \times 3.75^{\circ}$ ). The CAM3.1 has 26 vertical levels and CLM3.0 includes 10 soil layers. The Miocene vegetation is based on work by *Wolfe* [1985] with additional

<sup>1</sup>University of Sydney Institute of Marine Science, University of Sydney, New South Wales, Australia.

<sup>2</sup>School of Geosciences, University of Sydney, New South Wales, Australia.

<sup>3</sup>Department of Earth and Atmospheric Sciences, Purdue University, West Lafayette, Indiana, USA.

<sup>4</sup>Department of Geological Sciences, University of Michigan, Ann Arbor, Michigan, USA.

<sup>5</sup>Department of Biological and Physical Sciences, University of Southern Queensland, Toowoomba, Queensland, Australia.

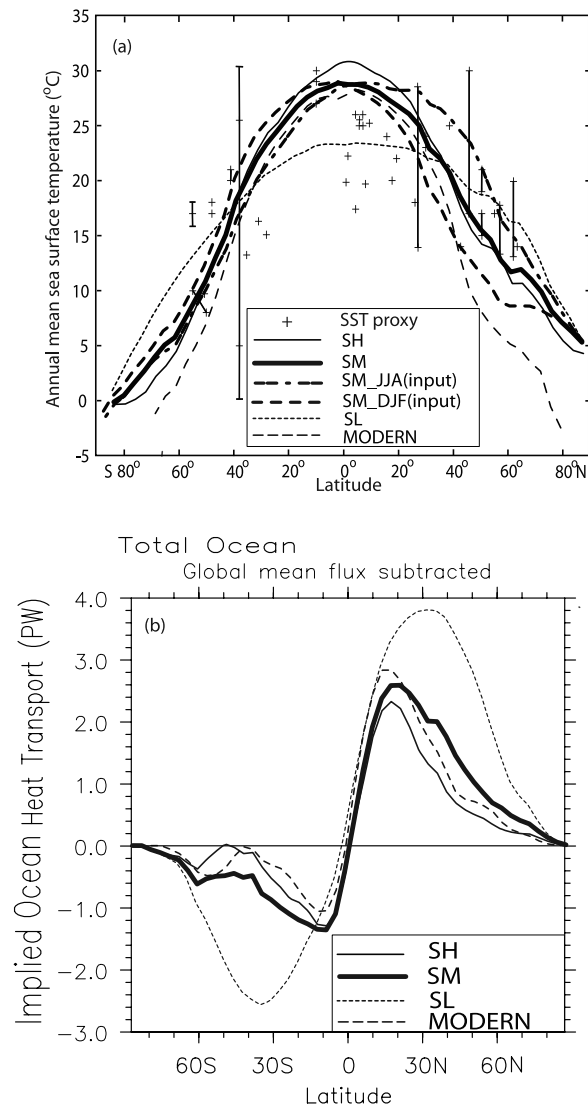


**Figure 1.** Zonal mean of (a) the simulated annual mean sea surface temperature ( $^{\circ}\text{C}$ ) for the scenarios SH (thin solid line), SM (thick solid line) and SL (short dashed line), compared with present (MODERN) (dashed line) and Miocene SST proxy (“+”): 1. *Shevenell et al.* [2004], 2. *Kershaw* [1997], 3. *Pagani et al.* [1999], 4. *Nikolaev et al.* [1998], 5. *Bojar et al.* [2005], 6. *Gonera et al.* [2000], 7. *Devereux* [1967], 8. *Van der Smissen and Rullkötter* [1996], 9. *Oleinik* [2001], 10. *Stewart et al.* [2004], 11. *Savin* [1975], 12. *Kobashi et al.* [2001], 13. *Savin* [1977] and 14. *Jenkins* [1968]; SM\_JJA (thick dash dotted line) and SM\_DJF (thick dashed line) represent summer and winter SST forcing input for the DOM model run and (b) the simulated northward ocean heat transport (PW) for the three Miocene scenarios and present.

detail for the Australian continent [*Christophel*, 1989]. To represent the absence of continental ice sheets during the Miocene, both Greenland and West Antarctic elevations have been reduced and land surface types have been modified to tundra. The East Antarctic remains ice covered with modern elevations. Sea ice is assumed to be absent

globally, given that none of the SST proxies infer temperatures below  $5^{\circ}\text{C}$ .

[7] Our middle Miocene paleotopography is constructed from the rotation of present day major tectonic plates back to 15 Ma, using the plate model from *Müller et al.* [2008]. We apply a maximum Tibetan Plateau elevation of 4700 m and a northern, central and southern Andes elevation of 500, 900 and 600 m, respectively. Maximum sea level in MMCO was estimated to have been about 100 m higher than present by *Haq and Al-Qahtani* [2005]; we use a conservative sea-level increase of about 50 m. In the absence of proxy data, greenhouse gas concentrations are set to preindustrial levels for methane (700 ppbv), nitrous oxide (275 ppbv), and chlorofluorocarbons (0 ppbv). The solar and orbital parameters are assumed to be constant for the middle Miocene period at 15 Ma and set to  $1.368\text{E}6 \text{ W m}^{-2}$  for the solar constant, 0.01492 for eccentricity, 181.0725 for precession and 23.46185 for obliquity [*Laskar et al.*, 2004]. The initial  $\text{CO}_2$  concentration is 700 ppmv in each of the scenarios referred to as high (SH\_700), medium (SM\_700) and low (SL\_700) gradient SST forcing.

[8] With the Miocene boundary conditions, the CAM3.1 coupled with CLM3.0 is initially integrated for 30 years with a data ocean model (DOM), which simply reads and interpolates the specified SST. This is necessary for the calculation of monthly ocean heat fluxes (i.e., Qflux), which are used in the subsequent slab ocean (SOM) runs. The model run is iterated, adjusting the low and high cloud relative humidity in CAM model code, until top-of-the-atmosphere and surface radiative balance is achieved, at which point the model is considered to be in equilibrium. The adjustment is necessary due to the change of initial and boundary conditions during MMCO so that radiative energy may be slightly imbalance. The last 10 years of the DOM run are used to calculate the Qflux. The CAM3.1 is then coupled with CLM3.0 and a slab ocean model (SOM), and run for 60 model years.

[9] In addition to our standard SH, SM, and SL cases with 700 ppmv  $\text{CO}_2$ , branch runs were completed for each SST scenario with  $\text{CO}_2$  concentrations reduced by approximately 50% to 350 and 180 ppmv. Branch runs were started from the end of our standard cases and iterated for 100 model years to attain equilibrium. In total, nine experiments were completed, three for each scenario: SH (SH\_700, SH\_350 and SH\_180); SM (SM\_700, SM\_350 and SM\_180) and SL (SL\_700, SL\_350 and SL\_180). To compare with the Miocene model results, a present day SOM run called MODERN is also carried out with  $\text{CO}_2$  355 ppmv and present boundary and initial conditions. In addition, a present day SOM experiment was run with Miocene orbital parameters to examine their effect on global surface temperatures. The mean of the last 10 years of each model run is presented here for analysis.

### 3. Results

[10] The simulated SSTs for the three scenarios, SH\_700, SM\_700 and SL\_700, are compared with present and proxy SSTs (Figure 1a). The SL SST (short dashed line) most closely matches proxy SST, as determined by a Gaussian best fit. In this simulation, low-latitude SSTs are about  $22^{\circ}\text{C}$ . Polar SSTs are more than  $10^{\circ}\text{C}$  higher than present

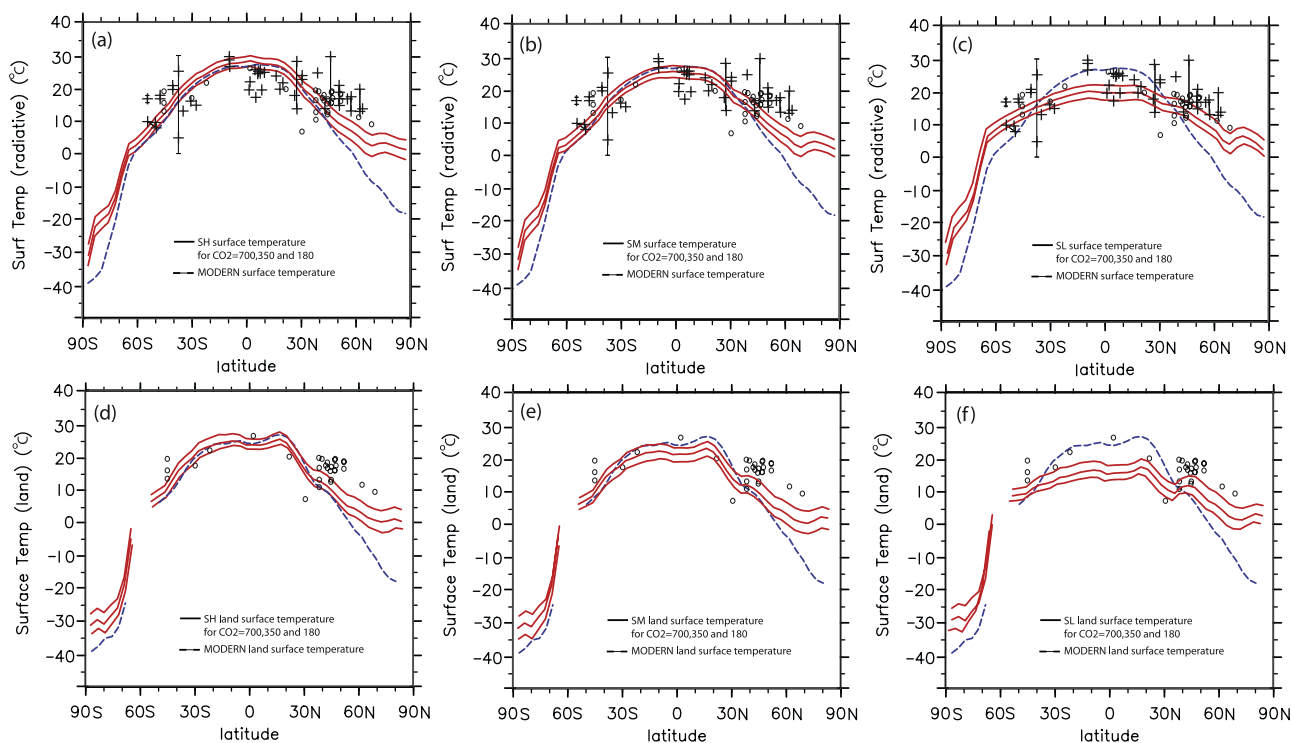


**Figure 2.** Simulated zonally averaged (top) annual mean surface temperature and (bottom) land only surface temperature for the three model scenarios (a and d) SH, (b and e) SM and (c and f) SL with  $\text{CO}_2$  concentrations from 700 ppmv to 350 and 180 ppmv, compared with the MODERN and Miocene SST proxy (pluses) (see Figure 1 caption for references) and land proxy (circles) (N. Herold, personal communication, 2008).

with an asymmetrical meridional distribution, a minimum of  $5^\circ\text{C}$  in Arctic and  $0.5^\circ\text{C}$  at Antarctica. The OHT of these simulations is examined in Figure 1b. Although the SL simulation best matches the proxy SST, the OHT is unrealistically large, approximately twice the modern heat transport, a result that is unlikely given current coupled modeling results [von der Heydt and Dijkstra, 2006]. This result indicates that to get a very low temperature gradient, and temperatures that match the magnitudes of proxy SST, high  $\text{CO}_2$  in addition to high OHT is necessary [Barron and Peterson, 1989; Huber and Sloan, 2001; Shellito et al., 2003; Sloan and Rea, 1995]. In contrast, the simulated OHT for SH and SM (in thin and thick solid lines) is similar to present. The SH has a peak tropical SST of about  $31^\circ\text{C}$  which is about  $3^\circ\text{C}$  higher than the present value of about  $28^\circ\text{C}$ . The SM tropical SST maximum is about  $29^\circ\text{C}$  only slightly higher than present.

[11] The simulated annual global mean surface temperature (top plots) and land-only surface temperature (bottom plots) are presented in Figure 2, and compared with the present value (dashed line) and proxies for Miocene SST (in cross) and land (in open circle). In each scenario, the simulated surface temperature decreases by about  $2^\circ$  and  $4^\circ\text{C}$ , respectively, with the rough 50% decrease in  $\text{CO}_2$ . The proxy surface temperature is best simulated in the SH and SM experiments with  $\text{CO}_2$  concentrations of 350 and 700 ppmv, respectively, as their global mean surface temperature is closest to the proxy mean temperature (see Figures 2a, 2b, 2d, and 2e). This comparison is further examined in Figure 3. In contrast, simulated surface tem-

perature in the SL cases is lower than marine and terrestrial proxies (Figures 2c and 2f), although SST is best matched in the first case above.

[12] In Figure 3, simulated global annual mean surface temperature is compared to the atmospheric  $\text{CO}_2$  concentrations. The global annual mean proxy surface temperature, including ocean and terrestrial data, is  $18.4^\circ\text{C}$ , about  $3^\circ\text{C}$  higher than that for the present-day simulation (asterisk). This represents the first assessment of the MMCO with a large distribution of proxy data used to estimate a global average temperature. Since most proxy data are found in mid latitudes, the simulated result gives more weight to those latitudes than high and low latitudes. The global average proxy temperature likely has an uncertainty of at least  $\pm 1^\circ\text{C}$ . Two simulations, SH\_350 and SM\_700, with a global mean temperature  $17.8^\circ\text{C}$  and  $19.0^\circ\text{C}$ , fall within this error range (about  $2.3^\circ\text{C}$  and  $3.5^\circ\text{C}$  higher than present, respectively). This is close to the difference between the proxy and present simulation ( $2.9^\circ\text{C}$ ). Interestingly, SH\_350 compares well because its land surface temperature ( $16.2^\circ\text{C}$ ) is almost the same as that derived from proxy data ( $16.1^\circ\text{C}$ ). Likewise, SM\_700 has a mean SST of  $20.5^\circ\text{C}$  which is about the same as the proxy-derived SST ( $20.6^\circ\text{C}$ ). The SL simulated mean SST's (in triangle, also see Figure 2) are generally too low. Although SL\_700 reaches the lower error bar ( $-1^\circ\text{C}$ ), the unrealistic OHT and poor comparison with proxy data, especially the land surface data (Figures 2c and 2f), render it unacceptable. However, even under relatively low  $\text{CO}_2$ , the mean surface temperatures are substantially higher than present with a



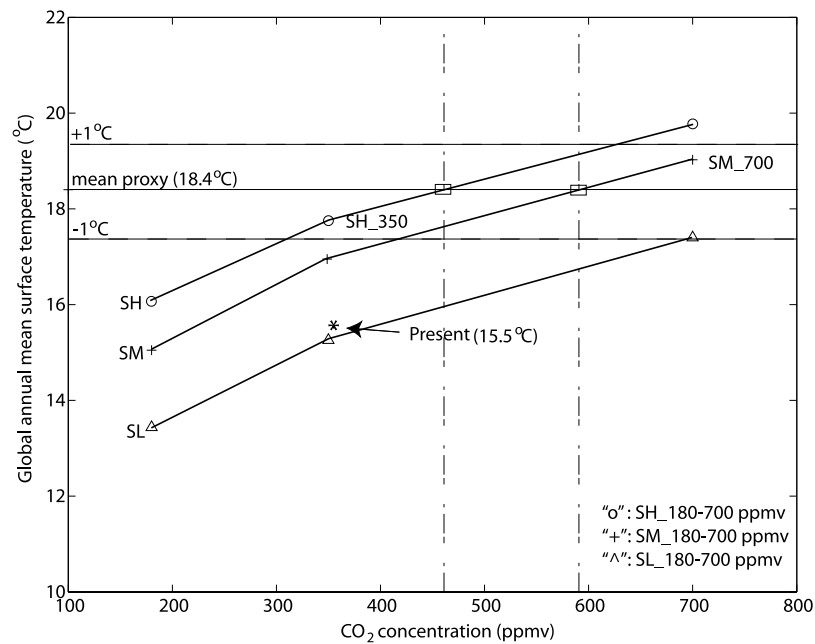


**Figure 3.** Simulated global annual mean surface temperature ( $^{\circ}\text{C}$ ) against  $\text{CO}_2$  concentrations (ppmv) for the three Miocene scenarios, SH (circles), SM (pluses) and SL (triangles), compared with present day simulation (asterisks) and mean proxy (thin solid line).

suitable SST forcing. The effect of MMCO orbital parameters on global mean surface temperature with respect to modern orbital parameters is small ( $-0.1^{\circ}\text{C}$ ).

#### 4. Discussion

[13] The issue of anomalously low Miocene tropical SST's derived from proxy data has been debated for some time. However a bias in proxy data may exist and is discussed here. The scattered tropical SST proxies are perhaps sampled through the same species of foraminifer shells, but under different conditions of diagenesis. Using well conserved foraminifer shells extracted from impermeable clay-rich sediments, *Pearson et al.* [2001] obtained tropical SST's of at least  $28^{\circ}$ – $32^{\circ}\text{C}$  in the Late Cretaceous and Eocene epochs, much higher than the  $15^{\circ}$ – $23^{\circ}\text{C}$  range estimated previously. *Poulsen et al.* [1999] and *Huber* [2008] discuss a number of issues that may cause low tropical SST estimates for past greenhouse intervals, associated with effects of diagenesis and assumptions of deep water properties for ancient seawater. A similar bias might apply to the MMCO proxy data. Another possibility is that planktonic foraminiferal preferentially grow during winter, thus recording lower seasonal temperature rather than mean-annual temperature [*Kobashi et al.*, 2001]. These factors are sufficient to explain the low tropical SST from proxy data (Figure 1a). In past model simulations, the “cool tropical paradox” and high subpolar SST's from proxies could not be reproduced [*Huber and Sloan*, 2001]. Many studies thus tend to agree that for most of the Tertiary the paleotropical SST should not differ from present by more than about  $2^{\circ}$ – $3^{\circ}\text{C}$  [*Adams et al.*, 1990; *Graham*, 1994].

[14] Except for some local bias especially in the northern mid-to-high latitudes, our model simulations are validated by a global averaged proxy surface temperature which has

reduced the probable bias to a minimum. However, the model-proxy-disagreement in part of the northern hemisphere latitudes may be due to the initial low meridional SST forcing input resulting in the simulated SST bias in mid-to-high latitudes in Figure 1a. On the other hand, the present-based-model may be less capable of simulating the asymmetrical meridional distribution of proxy surface temperature but more study is obviously needed in future. With Gaussian best fitting method of the SST proxy, our model fails to correctly simulate the OHT and surface temperatures. Successful simulations are achieved when the regression of the SST proxy is modified to match the maximum tropical temperatures while leaving the global mean SST value unchanged. This is done under the pretense that partial tropical Miocene proxies do not provide faithful temperature estimates. Our best simulations narrow the possible mid-Miocene atmospheric  $\text{CO}_2$  concentration from 300–600 ppmv to 460–580 ppmv. However, our simulation still lacks a dynamic ocean model which may further improve paleo-atmospheric  $\text{CO}_2$  simulations. Due to the limited space here we have not addressed other mechanisms to cause the MMCO warming such as the changes in global albedo, vegetation and altimetry which will be sought in future study.

[15] **Acknowledgments.** The project is supported by an Australian Research Council Discovery grant. We thank Nicholas Herold for providing the land proxy data. The model simulations were carried out on the APAC supercomputer in Canberra under a merit allocation scheme. Discussions with Bette Otto-Bliesner and Karen Bice were helpful. This work was initiated during the first author's visit to Purdue University.

#### References

Adams, C. G., D. E. Lee, and B. R. Rosen (1990), Conflicting isotopic and biotic evidence for tropical sea-surface temperatures during the Tertiary, *Palaeogeogr. Palaeoclimatol. Palaeoecol.*, 77, 289–313.

- Barron, E. J., and W. H. Peterson (1989), Model simulation of the Cretaceous ocean circulation, *Science*, *244*, 684–686.
- Bojar, A. V., H. Hiden, A. Fenninger, and F. Neubauer (2005), Middle Miocene temperature changes in the central paratethys: Relations with the East Antarctica ice sheet development, paper presented at South American Symposium on Isotope Geology, Dep. of Geol., Fed. Univ. of Pernambuco, Salvador, Brazil.
- Cerling, T. E. (1991), Carbon dioxide in the atmosphere: Evidence from Cenozoic and Mesozoic paleosols, *Am. J. Sci.*, *291*, 377–400.
- Christophel, D. C. (1989), Evolution of the Australian flora through the Tertiary, *Plant Syst. Evol.*, *162*, 63–78.
- Devereux, I. (1967), Oxygen isotope paleo-temperature measurements on New Zealand Tertiary fossils, *N. Z. J. Sci.*, *10*, 988–1011.
- Flower, B. P., and J. P. Kennett (1994), The middle Miocene climatic transition: East Antarctic ice sheet development, deep ocean circulation and global carbon cycling, *Palaeogeogr. Palaeoclimatol. Palaeoecol.*, *108*, 537–555.
- Graham, A. (1994), Neotropical Eocene coastal floras and  $^{18}\text{O}/^{16}\text{O}$ -estimated warmer vs. cooler equatorial waters, *Am. J. Bot.*, *81*, 301–306.
- Gonera, M., T. M. Peryt, and T. Durakiewicz (2000), Biostratigraphical and palaeoenvironmental implications of isotopic studies ( $^{18}\text{O}$ ,  $^{13}\text{C}$ ) of middle Miocene (Badenian) foraminifers in the Central Paratethys, *Terra Nova*, *12*(5), 231–238.
- Haq, B. U., and A. M. Al-Qahtani (2005), Phanerozoic cycles of sea-level change on the Arabian Platform, *GeoArabia*, *10*, 127–160.
- Huber, M. (2008), A hotter greenhouse?, *Science*, *321*, 353–354, doi:10.1126/science.1161170.
- Huber, M., and L. C. Sloan (2001), Heat transport, deep waters, and thermal gradients: Coupled simulation of an Eocene greenhouse climate, *Geophys. Res. Lett.*, *28*, 3481–3484.
- Huber, M., L. C. Sloan, and C. Shellito (2003), Early Paleogene oceans and climate: A fully coupled modeling approach using the NCAR CCSM, in *Causes and Consequences of Globally Warm Climates in the Early Paleogene*, edited by S. L. Wing et al., *Spec. Pap. Geol. Soc. Am.*, vol. 369, pp. 25–47.
- Jenkins, D. G. (1968), Variations in the number of species and subspecies of planktic foraminifera as an indicator of New Zealand Cenozoic paleotemperatures, *Palaeogeogr. Palaeoclimatol. Palaeoecol.*, *5*, 309–313.
- Kershaw, A. P. (1997), A bioclimatic analysis of early to middle Miocene brown coal floras, Latrobe valley, south-eastern Australia, *Aust. J. Bot.*, *45*, 373–387.
- Kobashi, T., E. L. Grossman, T. E. Yancey, and D. T. Dockery III (2001), Reevaluation of conflicting Eocene tropical temperature estimates: Molluscan oxygen isotope evidence for warm low latitudes, *Geology*, *29*, 983–986.
- Kürschner, W. M., Z. Kvaček, and D. L. Dilcher (2008), The impact of Miocene atmospheric carbon dioxide fluctuations on climate and the evolution of terrestrial ecosystems, *Proc. Natl. Acad. Sci. U. S. A.*, *105*, 449–453.
- Laskar, J., P. Robutel, F. Joutel, M. Gastineau, A. C. M. Correia, and B. Levrard (2004), A long-term numerical solution for the insolation quantities of the Earth, *Astron. Astrophys.*, *428*, 261–285.
- Müller, R. D., M. Sdrolias, C. Gaina, B. Steinberger, and C. Heine (2008), Long-term sea level fluctuations driven by ocean basin dynamics, *Science*, *319*, 1357–1362.
- Nikolaev, S. D., N. S. Oskina, N. S. Blyum, and N. V. Bubenshchikova (1998), Neogen-Quaternary variations of the 'pole-equator' temperature gradient of the surface oceanic waters in the North Atlantic and North Pacific, *Global Planet. Change*, *18*, 85–111.
- Oleinik, A. E. (2001), Biogeographic and stable isotope evidence for middle Miocene warming in the high-latitude North Pacific, paper presented at Annual Meeting, Geol. Soc. of Am., Boston, Mass.
- Pagani, M., M. A. Arthur, and K. H. Freeman (1999), Miocene evolution of atmospheric carbon dioxide, *Paleoceanography*, *14*, 273–292.
- Pearson, P. N., and M. R. Palmer (2000), Atmospheric carbon dioxide concentrations over the past 60 million years, *Nature*, *406*, 695–699.
- Pearson, P. N., P. W. Ditchfield, J. Singano, K. G. Harcourt-Brown, C. J. Nicholas, R. K. Olsson, N. J. Shackleton, and M. A. Hall (2001), Warm tropical sea surface temperatures in the late Cretaceous and Eocene epochs, *Nature*, *413*, 481–487.
- Poulsen, C. J., E. J. Barron, W. H. Peterson, and P. A. Wilson (1999), A reinterpretation of mid-Cretaceous shallow marine temperatures through model-data comparison, *Paleoceanography*, *14*, 679–697.
- Royer, D. L., S. L. Wing, D. J. Beerling, D. W. Jolley, P. L. Koch, L. J. Hickey, and R. A. Berner (2001), Paleobotanical evidence for near present-day levels of atmospheric  $\text{CO}_2$  during part of the Tertiary, *Science*, *292*, 2310–2313.
- Savin, S. M. (1977), The history of the Earth's surface temperature during the past 100 million years, *Annu. Rev. Earth Planet. Sci.*, *5*, 319–355.
- Savin, S. M., R. G. Douglas, and F. G. Stehli (1975), Tertiary marine paleotemperatures, *Geol. Soc. Am. Bull.*, *86*, 1499–1510.
- Shellito, C. J., L. C. Sloan, and M. Huber (2003), Climate model sensitivity to atmospheric  $\text{CO}_2$  levels in the Early Middle Paleogene, *Palaeogeogr. Palaeoclimatol. Palaeoecol.*, *193*, 113–123.
- Shevenell, A. E., J. P. Kennett, and D. W. Lea (2004), Middle Miocene Southern Ocean cooling and Antarctic cryosphere expansion, *Science*, *305*, 1766–1770, doi:10.1126/science.1100061.
- Sloan, L. C., and D. K. Rea (1995), Atmospheric carbon dioxide and early Eocene climate: A general circulation modeling sensitivity study, *Palaeogeogr. Palaeoclimatol. Palaeoecol.*, *119*, 275–292.
- Stewart, D. R. M., P. N. Pearson, P. W. Ditchfield, and J. M. Singano (2004), Miocene tropical Indian Ocean temperatures: Evidence from three exceptionally preserved foraminiferal assemblages from Tanzania, *J. Afr. Earth Sci.*, *40*, 173–190.
- Van der Smissen, J. H., and J. Rullkötter (1996), Organofacies variations in sediments from the central slope and rise of the New Jersey continental margin (sites 903 and 905), *Proc. Ocean Drill. Program Sci. Results*, *150*, 329–344.
- von der Heydt, A., and H. A. Dijkstra (2006), Effect of ocean gateways on the global ocean circulation in the late Oligocene and early Miocene, *Paleoceanography*, *21*, PA1011, doi:10.1029/2005PA001149.
- Wolfe, J. A. (1985), Distribution of major vegetational types during the Tertiary, in *The Carbon Cycle and Atmospheric  $\text{CO}_2$ : Natural Variations, Archaean to Present Geophys. Monogr. Ser.*, vol. 32, edited by E. T. Sundquist and W. S. Broecker, pp. 357–375, AGU, Washington, D. C.

M. Huber, Department of Earth and Atmospheric Sciences, Purdue University, West Lafayette, IN 47907, USA.

R. D. Müller, School of Geosciences, University of Sydney, NSW 2006, Australia.

C. J. Poulsen, Department of Geological Sciences, University of Michigan, Ann Arbor, MI 48109, USA.

J. Ribbe, Department of Biological and Physical Sciences, University of Southern Queensland, Toowoomba, Qld 4350, Australia.

Y. You, University of Sydney Institute of Marine Science, University of Sydney, NSW 2006, Australia. (you@geosci.usyd.edu.au)